Thermochimica Acta, 158 (1990) 125–141
Elsevier Science Publishers B.V., Amsterdam – Printed in The Netherlands

USING THERMOANALYTICAL DATA. PART 1. THE POWER OF KINETIC PARAMETERS DETERMINED FROM THERMOGRAVIMETRY TO DESCRIBE THE EXPERIMENTAL BEHAVIOUR OF THE SAMPLE

UGO BIADER CEIPIDOR

Istituto di Chimica, Università della Basilicata, Via N. Sauro, 85100-Potenza (Italy)

R. BUCCI *, V. CARUNCHIO and A.D. MAGRI

Dipartimento di Chimica, Università La Sapienza, P. le A. Moro, 00185-Roma (Italy)
(Received 10 July 1989)

ABSTRACT

Sources of misunderstandings when evaluating kinetic parameters from thermogravimetric (TG) curves are discussed. A simple method for calculating Arrhenius parameters, suitable for implementation on a PC connected to the TG apparatus, is presented. The results obtained with calcium oxalate are discussed with respect to their ability to predict thermal behaviour in several experimental conditions: agreement with experimental data is satisfactory. This is not so when using some literature-cited kinetic parameters, which fail to represent the same TG curves from which they are extracted. Suggestions are derived for design of a modern TG apparatus connected to a PC.

INTRODUCTION

Thermoanalytical methods are more and more frequently used to characterize materials [1], to obtain chemical and structural information [1,2] and, mainly, to predict material behaviour under extreme working conditions [3,4]. However, the strict dependence of the results obtained on experimental conditions often are not taken into account, even though the "fathers" of thermoanalysis clearly pointed out these constraints [5]. The reasons for this may be the difficulties of modelling the behaviour of a heated sample without a powerful calculating tool [6–10].

Possible misunderstandings were highlighted during the 9th ICTA (International Congress on Thermal Analysis) [11] together with the need to check, for instance, the predictive power of a kinetic model obtained from TG data. The goal of the present work can thus be summarized by the

* Author to whom correspondence should be addressed.

0040-6031/90/$03.50

following points. (i) Definition of a mathematical model of heat transfer during a TG experiment. (ii) Identification of parameters affecting kinetic measurements by TG. (iii) Implementation of a simple model for extracting kinetic parameters from TG measurements, in a way which is suitable for readily available PCs when connected to the TG apparatus. (iv) Checking the predictive power of the model on the thermal decomposition of calcium oxalate. (v) Discussion of the limits and significance of such an approach with respect to the use of obtained data. (vi) Introduction of some suggestions for refining the calculating procedure and for designing modern instruments.

EXPERIMENTAL

Thermogravimetric measurements were carried out using a Perkin–Elmer TGS-2 apparatus, in a dynamic nitrogen atmosphere flowing at 50 ml min^{-1}. TG data were collected and processed by a Perkin–Elmer 3700 Data Station operating in PETOS rev. D, using TADSOFT to read acquired data and BASIC rev. A to process the data. The calcium oxalate monohydrate was an analytical grade commercial product (from Carlo Erba RPE).

Model and symbols

When a solid sample S is heated it can react as follows

$$S \rightarrow P + G \tag{1}$$

where P is a solid product and G is the evolved gas. The kinetics of this reaction are generally assumed to obey the Arrhenius law in the form

$$-(dW/dt) = Z \exp(-E/RT) W^N \tag{2}$$

where W is the fraction of reagents present (or $1 - W$ is the extent of reaction), t is the time (s), T is the absolute temperature (K), R is the gas constant (J K^{-1} (apparent g mol)$^{-1}$), Z is the pre-exponential factor (s^{-1}), E is the activation energy in (J (apparent g mol)$^{-1}$) and N is the apparent order of reaction.

The simplest way to approach the measurement of W experimentally is to define it as follows

$$W = (m - m_f)/(m_i - m_f) \tag{3}$$

where m is the actual mass (at a given time), m_i is the initial mass, and m_f is the final mass.

The meaning of W, as well as $1 - W$ which is often used as the degree of reaction, can be understood physically when working under stoichiometric constraints. If M_S and M_P are the actual masses of S and P respectively

during the reaction, and if the stoichiometry implies that one mass unit of S gives b mass units of P ($b < 1$), then

$$m = M_S + M_P \tag{4}$$

$$m_i = M_S + M_P/b \tag{5}$$

$$m_f = m_i b \tag{6}$$

Using these relationships, W defined above corresponds to M_S/m_i whilst $1 - W$ corresponds to M_P/m_f, i.e. they represent linear relationships with respect to the mass of the reactant or of the product

$$W = (m - m_f)/(m_i - m_f) = (M_S + M_P - M_S b - M_P)/(m_i - m_i b)$$
$$= M_S/m_i \tag{7}$$

$$1 - W = (m_i - m)/(m_i - m_f) = (M_S + M_P/b - M_S - M_P)/(m_f/b - m_f)$$
$$= M_P/m_f \tag{8}$$

For the sample heating rate $B = dT/dt$ ($^\circ C\ s^{-1}$), the eqn. (2) may be rewritten as

$$-(dW/dT) = (Z/B)\exp(-E/RT)W^N \tag{9}$$

Assuming B to be constant during the reaction, i.e. equal to the controlled programmer heating rate B_p, it is possible to derive from eqn. (9) an expression for calculating Z, E and N from experimental TG curves, i.e. from a set of (W, T) couples identified as $W(i, j)$, $T(i, j)$ with $i = 1, \cdots, N_j$ for N_j points for each jth curve

$$\log(-D_W/D_T) + \log B = \log Z - (E/2.3R)(1/T) + N \log W \tag{10}$$

where

$$D_W = W(i, j) - W(i-1, j) \tag{11}$$

$$D_T = T(i, j) - T(i-1, j) \tag{12}$$

$$W = W(i, j) \tag{13}$$

$$T = T(i, j) \tag{14}$$

$$B = B(j) \tag{15}$$

Provided that the set of (W,T) couples gives values sufficiently close to allow numerical differentiation (many close points are available when a PC is connected to the TG instrument), it is possible to make a linear regression analysis of $\log(-D_W/D_T) + \log B$ vs. $1/T$ and $\log W$ and to calculate Z, E and N. In the present work, kinetic parameters were calculated in this way, by first choosing a given reaction step, then slightly smoothing the experimental curves and finally by performing least-squares linear regression analysis in a selected W range (generally 98–2% for reducing the contribution of points where the numerical derivatives approach zero).

The above method is based, as others [6–10,12,13], on the assumption that the sample temperature is very close to the external programmer temperature, and that the sample heating rate B is constant. In practice only the programmer (heater) heating rate B_p is constant whilst the sample heating rate B is not. Consequently, the programmer temperature (measured by the instruments) does not correspond to the sample temperature. Even when the measured temperature is "that of the sample", i.e. obtained from a probe very close to the sample itself, heat flow between sample and probe must be considered. In this case the difference between sample temperature and the measured temperature is slightly reduced, but still exists.

In addition to eqn. (2), a more realistic representation of the sample temperature could be derived, when considering also an energy balance between $Q1$ (heat per unit time transferred between the environment, i.e. the programmer or the controlled heater, and the sample holder) and $Q2$ (heat absorbed or evolved per unit time to increase or decrease the holder and sample temperature and to balance reaction enthalpy). The heat flows $Q1$ and $Q2$ may be expressed as functions $FNM(\ldots,\ldots)$ of operational parameters

$$Q1 = F11(k,\ T_p - T) \tag{16}$$

$$Q2 = F21(CT_{,0},\ \mathrm{d}T/\mathrm{d}t) + F22(m,\ C_s,\ \mathrm{d}T/\mathrm{d}t) + F23(m,\ H,\ \mathrm{d}W/\mathrm{d}t) \tag{17}$$

where k represents a set of transfer coefficients, T_p is the programmer temperature, T is the temperature of the sample, assumed to be the same as that of the holder, $CT_{,0}$ is the thermal capacity of the holder, m is the mass reacting, C_s is the specific heat of the mass reacting, H is the reaction enthalpy and t is the time. Regardless of the explicit form of the operational functions $F11$ and $F21$–$F23$, some considerations must be taken into account: $F11$, as a general flow promoted by the driving force $T_p - T$, is reduced to zero when T approaches T_p; $F21$ and $F22$, as heats spent to increase temperature, are reduced to zero when $\mathrm{d}T/\mathrm{d}t$ approaches zero; $F22$ and $F23$, which are connected with the sample, are reduced to zero when the mass m approaches zero.

By equating $Q1$ and $Q2$, as an energy balance, and taking into account the above considerations, the following relationship can be derived

$$T_p - T = (\mathrm{d}T/\mathrm{d}t)A1 + mA2 \tag{18}$$

where $A1$ and $A2$ represent coefficients which depend on all the variables describing $F11$ and $F21$–$F23$, i.e. k, $CT_{,0}$, m, C_s, H, T, $\mathrm{d}T/\mathrm{d}t$, $\mathrm{d}W/\mathrm{d}t$.

If T_p is considered to be an independent variable, i.e. the abscissa, eqn. (10) may be rewritten

$$\log\left[\left(-D_W/D_{T_p}\right)\left(D_{T_p}/D_T\right)\right] + \log B = \log Z - (E/2.3R)\left[1/\left(T_p + \left(T - T_p\right)\right]\right] + N \log W \tag{19}$$

Using the approximations

$$D_{T_p}/D_T \approx (\mathrm{d}T_p/\mathrm{d}t)(\mathrm{d}t/\mathrm{d}T) = B_p/B \tag{20}$$

$$1/\left[T_p + (T - T_p)\right] = 1/\left\{T_p\left[1 + (T - T_p)/T_p\right]\right\} \approx (1/T_p)\left[1 + (T_p - T)/T_p\right] \tag{21}$$

eqn. (19) becomes

$$\log\left(-D_W/D_{T_p}\right) + \log B_p) = \log Z - (E/2.3R)(1/T_p) + N \log W - (E/2.3R)(T_p - T)/T_p^2 \tag{22}$$

where the symbols have the same meanings as in eqn. (10), with the addition of $D_{T_p} = T_p(i, j) - T_p(i-1, j)$, $T_p = T_p(i, j)$ and $B_p = B_p(j)$.

As shown by eqn. (18), the sample temperature T approaches T_p, and $B = \mathrm{d}T/\mathrm{d}t$ approaches $B_p = \mathrm{d}T_p/\mathrm{d}t$ (constant instrumental heating rate), at the point where the sample mass and/or heating rate are sufficiently low. Under this condition the last term in eqn. 22 can be neglected and this can then be used to calculate kinetic parameters, being similar to eqn. (10). When the above condition is not satisfied, eqn. (22) will allow the calculation of kinetic parameters provided that $T_p - T$ is also recorded.

RESULTS

In Figs. 1–3 the experimental TG curves of calcium oxalate are given as W versus T for two sample masses and two heating rates for the three

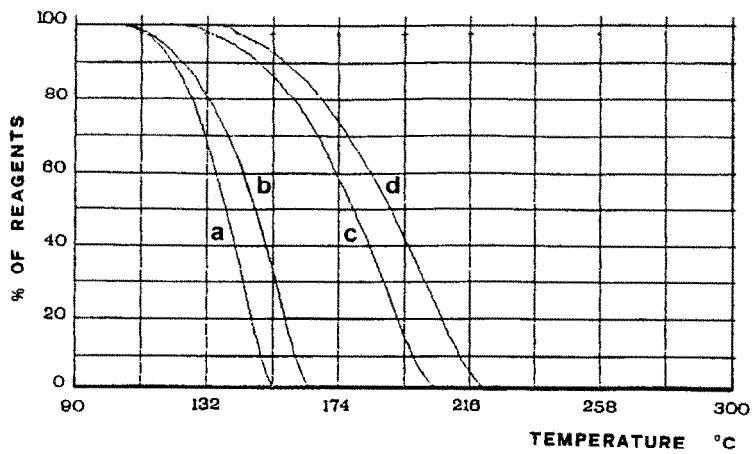

Fig. 1. Experimental TG curves for reaction step 1: dehydration of calcium oxalate monohydrate. $W = (m - m_f)/(m_i - m_f)$; T is the programmer temperature in °C; B is the programmer heating rate in °C min^{-1}; m_i and m_f are the initial and final mass, respectively, in mg. Curve a, $m_i = 10.0$, $m_f = 8.8$, $B = 2.5$; curve b, $m_i = 20.1$, $m_f = 17.6$, $B = 2.5$; curve c, $m_i = 10.0$, $m_f = 8.8$, $B = 20$; curve d, $m_i = 20.0$, $m_f = 17.5$, $B = 20$.

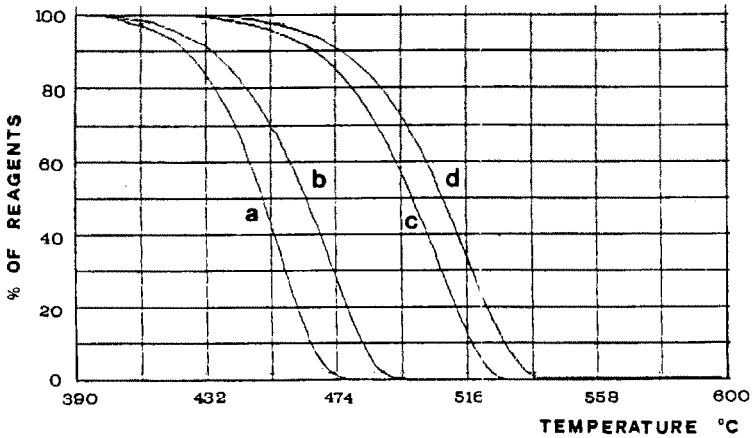

Fig. 2. Experimental TG curves for reaction step 2: decomposition of calcium oxalate. W $(m - m_f)/(m_i - m_f)$; T is the programmer temperature in °C; B is the programmer heating rate in °C min^{-1}; m_i and m_f are the initial and final mass, respectively in mg. Curve a, $m_i = 8.7$, $m_f = 6.9$, $B = 2.5$; curve b, $m_i = 17.5$, $m_f = 13.7$, $B = 2.5$; curve c, $m_i = 8.7$, $m_f = 6.9$, $B = 20$; curve d, $m_i = 17.4$, $m_f = 13.7$, $B = 20$.

reaction steps

$$CaC_2O_4 \cdot H_2O \rightarrow CaC_2O_4 + H_2O\uparrow \quad \text{(step 1)}$$

$$CaC_2O_4 \rightarrow CaCO_3 + CO\uparrow \quad \text{(step 2)}$$

$$CaCO_3 \rightarrow CaO + CO_2\uparrow \quad \text{(step 3)}$$

Figures 4–6 show calculated TG curves corresponding to the experimen-

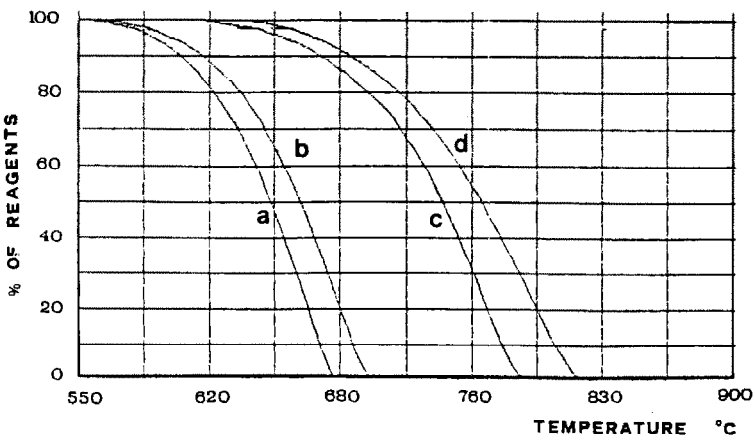

Fig. 3. Experimental TG curves for reaction step 3: decomposition of calcium carbonate. $W = (m - m_f)/(m_i - m_f)$; T is the programmer temperature in °C; B is the programmer heating rate in °C min^{-1}; m_i and m_f are the initial and final mass, respectively in mg. Curve a, $m_i = 6.9$, $m_f = 3.9$, $B = 2.5$; curve b, $m_i = 13.6$, $m_f = 7.7$, $B = 2.5$; curve c, $m_i = 6.8$, $m_f = 3.9$, $B = 20$; curve d, $m_i = 13.6$, $m_f = 7.7$, $B = 20$.

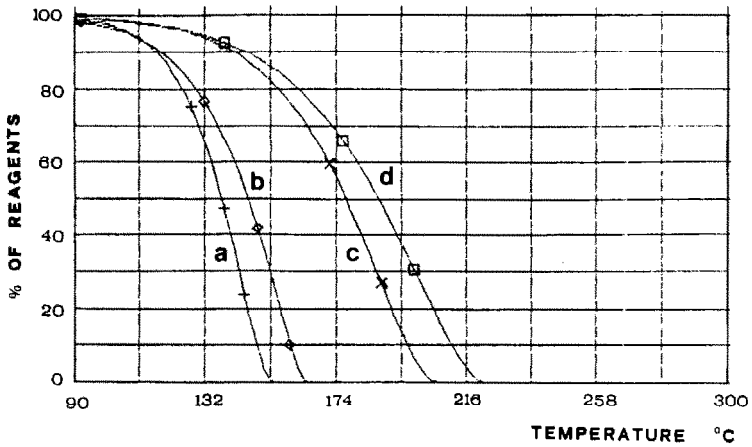

Fig. 4. Calculated TG curves for reaction step 1: dehydration of calcium oxalate monohydrate. The kinetic parameters from the best-fit of the corresponding curves in Fig. 1 are Z (s^{-1}), E (kJ mol^{-1}) and N. Curve a, $Z = 1.84 \times 10^{12}$, $E = 117.4$, $N = 0.597$; curve b, $Z = 1.02 \times 10^{7}$, $E = 79.2$, $N = 0.365$; curve c, $Z = 1.17 \times 10^{6}$, $E = 70.0$, $N = 0.530$; curve d, $Z = 4.05 \times 10^{4}$, $E = 59.5$, $N = 0.500$.

tal ones of Figs. 1–3. These are calculated by integration of eqn. (9) using kinetic parameters obtained through linear regression (best-fit) of eqn. (10), applied to each TG curve of Figs. 1–3. The figure legends give the values of the kinetic parameters.

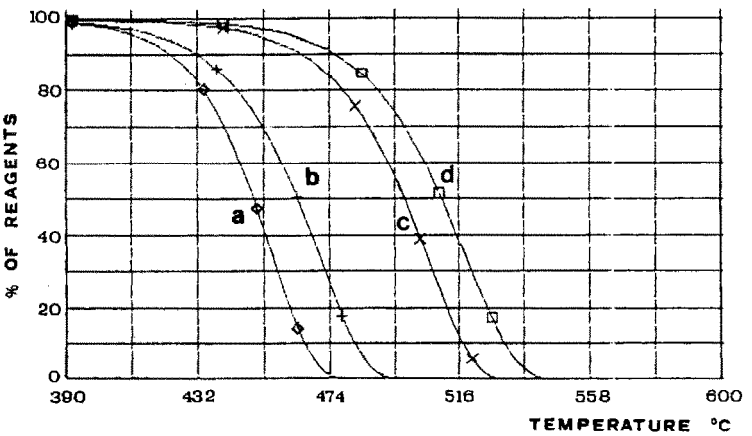

Fig. 5. Calculated TG curves for reaction step 2: decomposition of calcium oxalate. The kinetic parameters from the best-fit of the corresponding curves in Fig. 2 are Z (s^{-1}), E (kJ mol^{-1}) and N. Curve a, $Z = 6.42 \times 10^{17}$, $E = 284.5$, $N = 0.807$; curve b, $Z = 1.05 \times 10^{14}$, $E = 238.0$, $N = 0.716$; curve c, $Z = 5.45 \times 10^{14}$, $E = 246.8$, $N = 0.685$; curve d, $Z = 1.60 \times 10^{14}$, $E = 242.9$, $N = 0.715$.

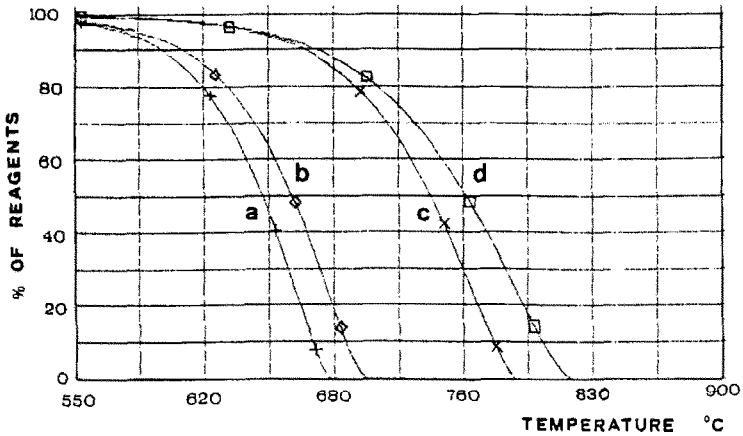

Fig. 6. Calculated TG curves for reaction step 3: decomposition of calcium carbonate. The kinetic parameters from the best-fit of the corresponding curves in Fig. 3 are Z in (s^{-1}), E in (kJ mol^{-1}) and N. Curve a, $Z = 1.40 \times 10^8$, $E = 200.1$, $N = 0.368$; curve b, $Z = 2.41 \times 10^7$, $E = 190.4$, $N = 0.374$; curve c, $Z = 1.98 \times 10^7$, $E = 187.6$, $N = 0.382$; curve d, $Z = 4.51 \times 10^5$, $E = 160.2$, $N = 0.397$.

From linear regression analysis of all available data (see Figs. 1–3) other values are obtained. The ability of these latter values to represent the experimental curves is shown in Figs. 7–9.

Calculated TG curves obtained using kinetic parameters from ref. 14, as an example of recent literature data, are given in Figs. 10–12. Those obtained using the data processing method supplied with the TG instrument used in this work are given in Figs. 13–15.

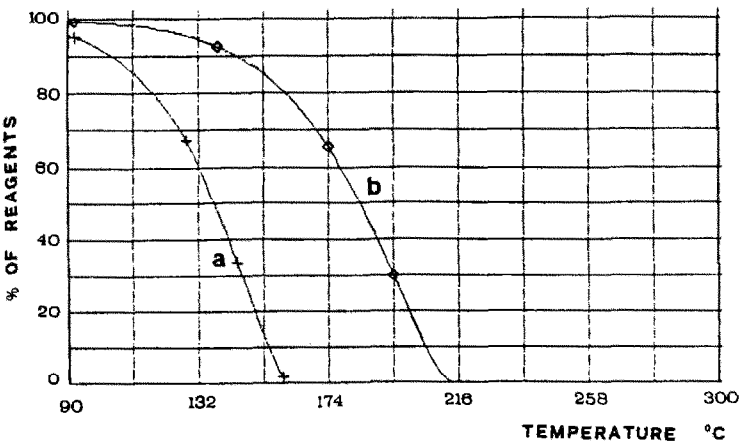

Fig. 7. Calculated TG curves for reaction step 1: dehydration of calcium oxalate monohydrate. The kinetic parameters from the simultaneous best-fit of all the curves in Fig. 1 are reported in Table 1, BF2. Curve a, $B = 2.5\,^{\circ}C\ min^{-1}$; curve b, $B = 20\,^{\circ}C\ min^{-1}$.

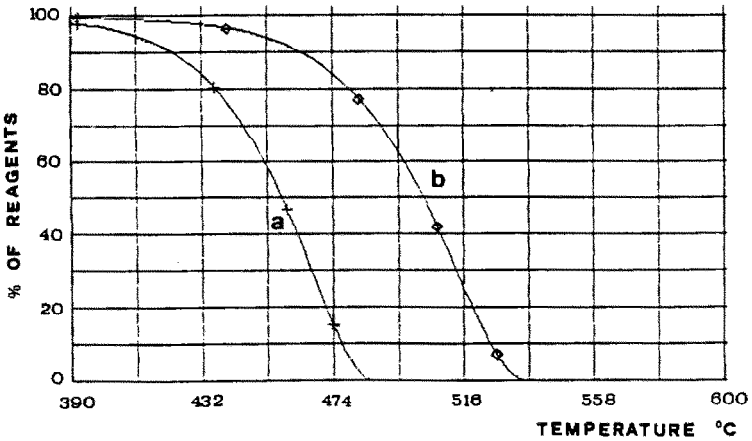

Fig. 8. Calculated TG curves for reaction step 2: decomposition of calcium oxalate. The kinetic parameters from the simultaneous best-fit of all the curves in Fig. 2 are reported in Table 1, BF2. Curve a, $B = 2.5\,^{\circ}\mathrm{C\ min^{-1}}$; curve b, $B = 20\,^{\circ}\mathrm{C\ min^{-1}}$.

The complete set of kinetic parameters, together with other literature data, is summarized in Table 1 to allow direct comparison. In ref. 15 there is no direct evidence of pre-exponential factors, so those calculated by other authors [16] were used. Sources of data are given in the column headings: BF1 is the best-fit of eqn. (10) applied to the TG curves at the lower mass and heating rate, i.e. 10 mg and $2.5\,^{\circ}\mathrm{C\ min^{-1}}$; BF2 is the same applied to all the reported curves; PE is calculation using the Perkin–Elmer data processing method supplied with the instrument, using all the reported curves and two

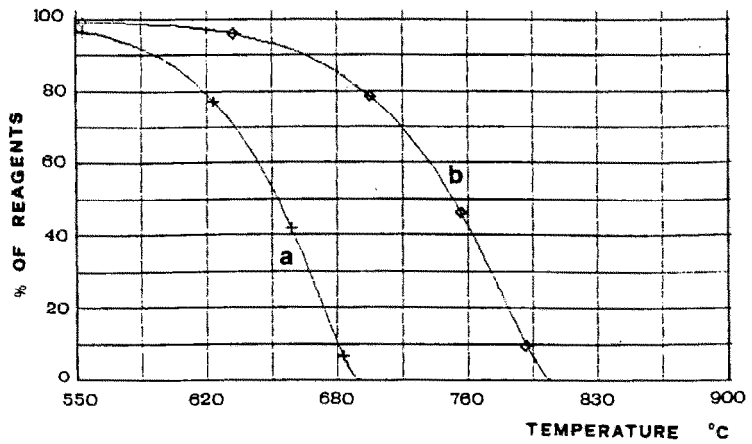

Fig. 9. Calculated TG curves for reaction step 3: decomposition of calcium carbonate. The kinetic parameters from the simultaneous best-fit of all the curves in Fig. 3 are reported in Table 1, BF2. Curve a, $B = 2.5\,^{\circ}\mathrm{C\ min^{-1}}$; curve b, $B = 20\,^{\circ}\mathrm{C\ min^{-1}}$.

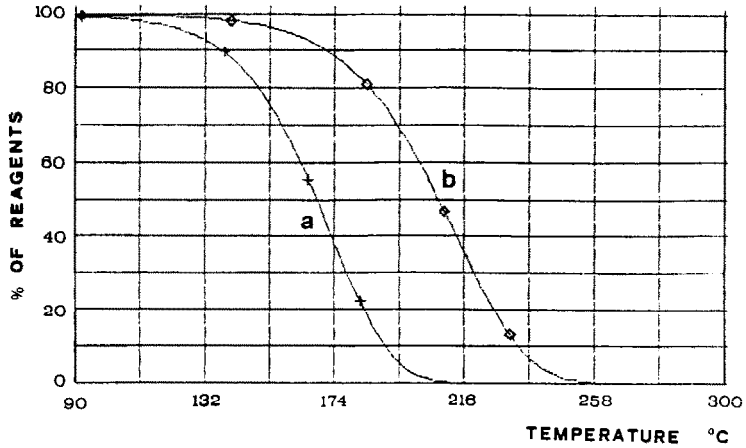

Fig. 10. Calculated TG curves for reaction step 1: dehydration of calcium oxalate monohydrate. The kinetic parameters are from ref. 14. Curve a, $B = 2.5\,^{\circ}\mathrm{C\ min^{-1}}$; curve b, $B = 20\,^{\circ}\mathrm{C\ min}$.

others recorded with 10 mg at $10\,^{\circ}\mathrm{C\ min^{-1}}$ and 10 mg at $40\,^{\circ}\mathrm{C\ min^{-1}}$, at 20% conversion; R14, R15 and R16 are literature data from refs. 14–16.

DISCUSSION

The best-fit of eqns. (10) or (22) allows calculation of kinetic parameters from a single TG curve, as well as from many curves at different heating rates and/or masses.

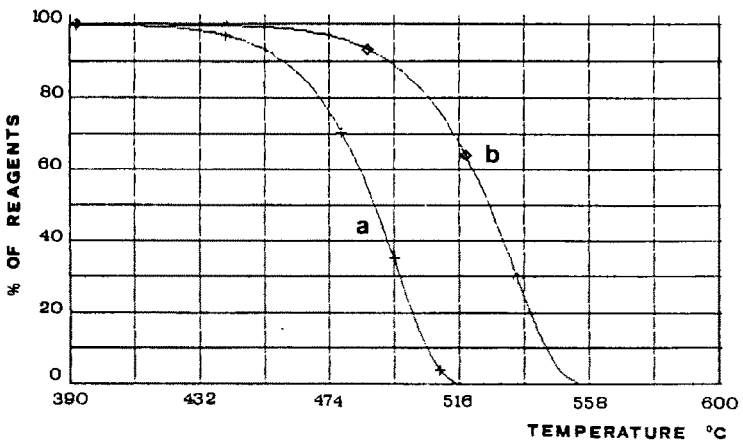

Fig. 11. Calculated TG curves for reaction step 2: decomposition of calcium oxalate. The kinetic parameters are from ref. 14. Curve a, $B = 2.5\,^{\circ}\mathrm{C\ min^{-1}}$; curve b, $B = 20\,^{\circ}\mathrm{C\ min^{-1}}$.

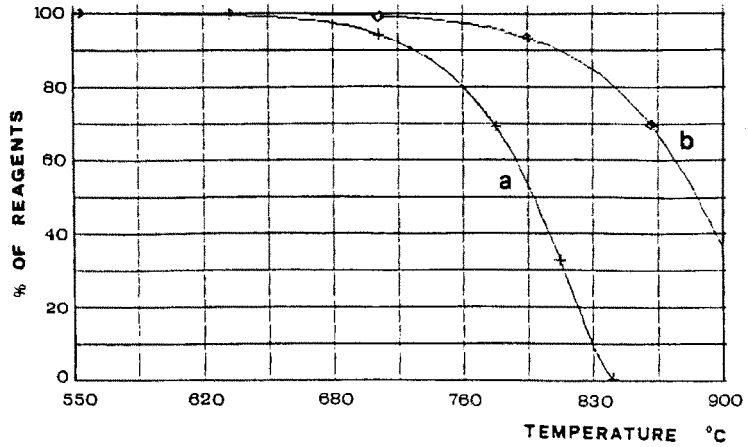

Fig. 12. Calculated TG curves for reaction step 3: decomposition of calcium carbonate. The kinetic parameters are from ref. 14. Curve a, $B = 2.5\,^{\circ}\mathrm{C\ min^{-1}}$; curve b, $B = 20\,^{\circ}\mathrm{C\ min^{-1}}$.

When Figs. 4–6 are compared with Figs. 1–3, a good agreement is found even if the kinetic parameters differ considerably (depending on the curves used to calculate them). This accounts for a good self-predictive power, i.e. the ability to reconstruct the original TG curves. This is not a poor result when observing other values which fail [14]. From the complete set of TG curves a unique triplet of kinetic parameters may be obtained. However, the predictive power, i.e. the ability to describe all the TG curves, is reduced as shown by a comparison of Figs. 7–9 with Figs. 1–3. Differences from the experimental curves in Figs. 1–3 become more relevant when considering

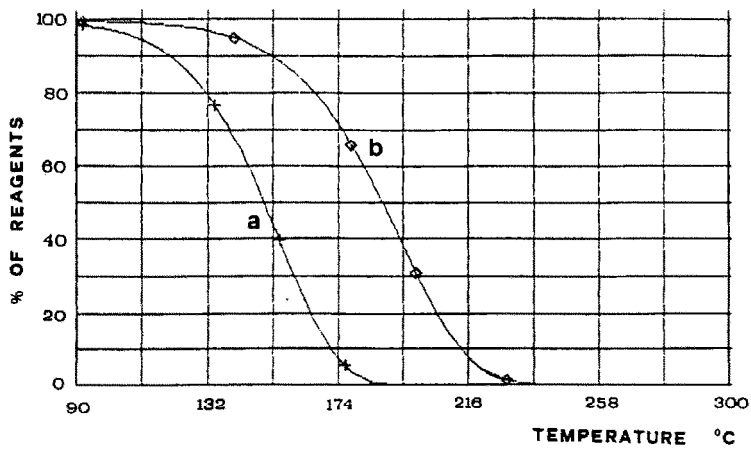

Fig. 13. Calculated TG curves for reaction step 1: dehydration of calcium oxalate monohydrate. The kinetic parameters are from Perkin–Elmer data processing of curves 1a–1d plus two others (see text) at 20% reaction (reported in Table 1 as PE). Curve a, $B = 2.5\,^{\circ}\mathrm{C\ min^{-1}}$; curve b, $B = 20\,^{\circ}\mathrm{C\ min^{-1}}$.

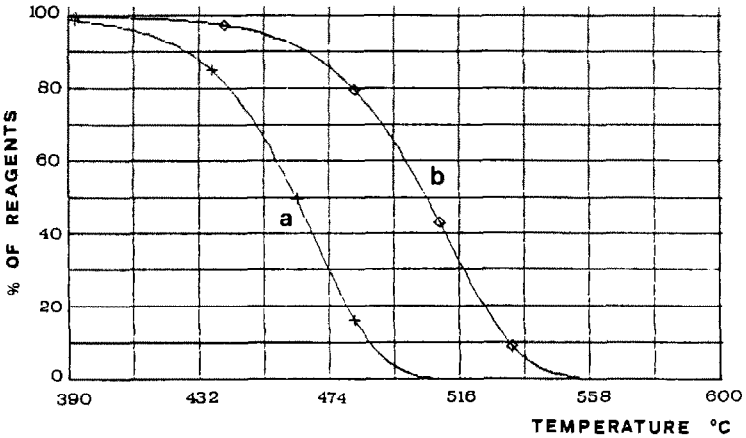

Fig. 14. Calculated TG curves for reaction step 2: decomposition of calcium oxalate. The kinetic parameters are from Perkin–Elmer data processing of curves 2a–2d plus two others (see text) at 20% reaction (reported in Table 1 as PE). Curve a, $B = 2.5\,^{\circ}\mathrm{C\ min^{-1}}$; curve b, $B = 20\,^{\circ}\mathrm{C\ min^{-1}}$.

curves calculated from literature data (Figs. 10–12), whilst those produced using the Perkin–Elmer data processing method (Figs. 13–15) are slightly more displaced.

A simple residual standard deviation is not suitable for expressing quantitatively the ability of the calculated curves to represent the experimental curves (predictive power). This is because the squaring of differences causes the direction of the shift to disappear. In particular, the predictive power of curves which are shifted with respect to the experimental curves

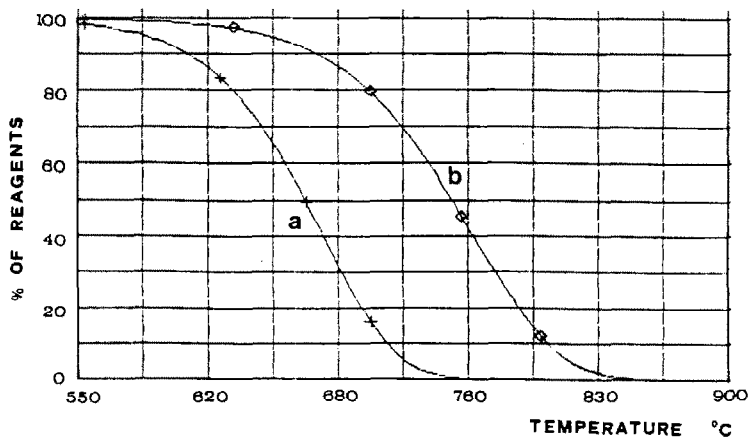

Fig. 15. Calculated TG curves for reaction step 3: decomposition of calcium carbonate. The kinetic parameters are from Perkin–Elmer data processing of curves 3a–3d plus two others (see text) at 20% reaction (reported in Table 1 as PE). Curve a, $B = 2.5\,^{\circ}\mathrm{C\ min^{-1}}$; curve b, $B = 20\,^{\circ}\mathrm{C\ min^{-1}}$.

TABLE 1

Kinetic parameters for the three steps of the thermal decomposition of calcium oxalate according to several sources. Residual standard errors are reported in parenthesis for data obtained in this work

	BF1	BF2	R14	PE	R16 [a]	R15
Step 1						
Z (s^{-1})	1.84×10^{12} (1.78×10^{12})	9.24×10^{4} (4.07×10^{4})	2.43×10^{7}	1.77×10^{7}	4.33×10^{4}	2.80×10^{6}
E (kJ mol^{-1})	117.4 (3.6)	62.1 (1.8)	86.0	81.2	63.0	92.1
N	0.597 (0.035)	0.404 (0.030)	1	1	0.63	1
Step 2						
Z (s^{-1})	6.42×10^{17} (3.39×10^{17})	4.34×10^{11} (3.14×10^{11})	7.27×10^{15}	9.11×10^{12}	7.27×10^{15}	2.33×10^{15}
E (kJ mol^{-1})	284.5 (3.4)	203.7 (4.8)	272.6	222.6	258.4	309.8
N	0.807 (0.017)	0.579 (0.030)	0.7	1	0.75	0.7
Step 3						
Z (s^{-1})	1.40×10^{8} (0.56×10^{8})	5.55×10^{5} (1.90×10^{5})	7.14×10^{7}	5.70×10^{7}	2.77×10^{8}	4.33×10^{7}
E (kJ mol^{-1})	200.1 (3.5)	160.4 (3.0)	227.3	196.3	201.1	163.3
N	0.368 (0.022)	0.358 (0.023)	0.4	1	0.36	0.4

[a] The Z reported values for steps 1 and 2 were considered to be in units of min^{-1}: if in s^{-1} as for the other reported values agreement with experimental data fails extensively (the curves are displaced toward higher temperatures by hundreds of degrees).

could be evaluated as being similar to the predictive power of curves which cross the experimental curves. In fact, the latter are better than the former for predicting the behaviour of the sample.

To give a quantitative representation whilst taking account of the above restriction, the difference between calculated and experimental curves are reported in Table 2 as temperature differences at the points where the extents of reaction are 25% ($W = 0.75$), 50% ($W = 0.5$) and 75% ($W = 0.25$). The sources of the kinetic parameters are as given in Table 1.

The best agreement with experimental data is displayed by BF1 with respect to the a curves. This accounts for the self-predictive ability of the model, i.e. giving data from which kinetic parameters may be derived. However, this is not a measure of the predictive power in a wide range of experimental conditions. Looking at all data, the predictive power shows the sequence BF2 > PE > BF1 > R16 > R14 > R15. The relationship between BF2 and BF1 is obvious since BF2 uses all the curves whilst BF1 only uses

TABLE 2

Temperature differences between experimental TG curves for the three steps of the thermal decomposition of calcium oxalate and those calculated using different sources for kinetic parameters at extents of reaction of 25%, 50% and 75% curves a, 10 mg, 2.5 °C min^{-1}; curves b, 20 mg, 2.5 °C min^{-1}; curves c, 10 mg, 20 °C min^{-1}; curves d, 20 mg, 20 °C min^{-1}. The symbols $\ll$ and $\gg$ indicate values much less than zero and much greater than zero respectively.

		BF1	BF2	R14	PE	R16	R15	Experimental values of T (°C)
Curves a								
Step 1	25%	−0	6	−25	−7	−15	−95	129
	50%	−0	0	−31	−13	−23	−105	138
	75%	−1	−4	−37	−19	−30	−114	144
Step 2	25%	1	−3	−37	−8	1	−158	439
	50%	−1	−8	−40	−14	−1	$\ll$	450
	75%	−1	−11	−41	−18	−2	$\ll$	459
Step 3	25%	2	1	−141	−13	19	$\gg$	630
	50%	1	−5	−146	−19	19	$\gg$	654
	75%	1	−10	−150	−28	19	$\gg$	670
Curves b								
Step 1	25%	6	12	−19	−1	−9	−89	135
	50%	9	9	−22	−4	−14	−96	147
	75%	11	8	−25	−7	−18	−102	156
Step 2	25%	12	8	−26	3	12	−147	450
	50%	14	7	−25	1	14	$\ll$	465
	75%	17	7	−23	−0	16	$\ll$	477
Step 3	25%	17	16	−126	2	34	$\gg$	645
	50%	17	11	−130	−3	35	$\gg$	670
	75%	18	7	−133	−11	36	$\gg$	687
Curves c								
Step 1	25%	9	−4	−29	−10	−30	−109	162
	50%	15	−7	−30	−11	−35	−115	178
	75%	20	−8	−33	−13	−39	$\ll$	190
Step 2	25%	16	−1	−27	−3	13	$\ll$	485
	50%	18	−4	−27	−6	14	$\ll$	500
	75%	17	−7	−28	−11	13	$\ll$	510
Step 3	25%	16	−2	$\ll$	−2	36		715
	50%	18	−8	$\ll$	−7	39		745
	75%	19	−13	$\ll$	−16	41		765
Curves d								
Step 1	25%	19	6	−19	0	−20	−99	172
	50%	27	5	−18	1	−23	−103	190
	75%	33	5	−20	−0	−26	$\ll$	203
Step 2	25%	24	7	−19	5	21	$\ll$	493
	50%	27	5	−18	3	23	$\ll$	509
	75%	29	5	−16	1	25	$\ll$	522
Step 3	25%	33	15	$\ll$	15	53		732
	50%	38	12	$\ll$	13	59		765
	75%	44	12	$\ll$	9	66		790

the a curves. PE also uses all the curves and so gives better results than BF1. A particularly good agreement is found for the b and d curves, where the mass and heating rate perturbations of eqn. (22), induced by eqn. (18), are higher: this is a result of the fact that two more curves, at higher heating rates, were used to improve the linear regression analysis from 4 to 6 points. In such a way, the 'weight' of the results from perturbated curves were increased and consequently the kinetic parameters obtained better describe the above curves. The poor agreement of R16 could arise from a difference in the experimental conditions even if Z values were held to be in units of min^{-1} for step 1 and step 2 (other Z values are reported in units of s^{-1}). Using the other sources, the calculated curves lie so far from the experimental data that the only possible interpretation is that the experimental data are wrong or are reported in a misleading form in ref. 16. The fact that the predictive power of BF1 decreases from the a curves to the d curves, whilst the predictive powers of the other curves are randomly distributed, is a result of the effect of heat transfer described by eqn. (18): when kinetic parameters are obtained from data at a lower mass and heating rate they are affected less by perturbation of the model. However, when the same parameters are obtained by 'mixing' data at higher masses and heating rates these parameters contain the perturbation and adapt themselves to describe the complete set of data, thus becoming different from the 'true' parameters. This situation is common to all methods which employ more than one TG curve to calculate parameters.

By comparing for example the BF2 kinetic parameters with the PE kinetic parameters (Table 1), it may be seen that a similar reconstruction could also occur when using a different set of parameters, both sets being 'true' with respect to representation of curves. The values obtained with BF1 and BF2 have small residual standard errors, thus confirming the good linear fit of eqn. (10). (The apparent high residual standard errors of Z values are caused by the representation being linear whilst the calculation, as for E and N, is logarithmic: $2.3S\ (\log x) = S(x)/x$.) Table 1 also shows that the differences between BF1 and BF2 values become lower when passing from step 1 to step 2 to step 3. This observation agrees with eqn. (22) if the perturbation induced by the last term is considered to be lowered as T_p values in the range examined become larger. Consequently, a combination of data obtained at different heating rates approaches a single curve processing, as kinetic parameters approach the 'true' ones.

It has been shown above that triplets (Z, E, N) having an acceptable agreement with experimental data, defined as 'true', could have different individual values. The approach used is simply a method of empirically representing a complex process with a simple relationship (eqn. (2)). The common reporting of just two kinetic parameters, as Z and E or E and N, could thus give no useful result because of their inability to represent data. Any attempt to assign chemical significance to kinetic parameters, such as

activation energy or order of reaction, may fail not only because eqn. (2) cannot match the real chemical process [12,17], but also because eqn. (18) would need to be considered also. In conditions where sample mass and heating rate are sufficiently low eqn. (18) can be ignored and consequently eqn. (22) is not influenced by the final term and so becomes similar to eqn. (10). Thus the best values for describing the thermal decomposition of calcium oxalate are those reported in Table 1 in column BF1.

Limiting the best-fit range to W values approaching unity, i.e. $0.99 < W < 0.70$, also reduces the contribution of eqn. (18) because of limited evolved or absorbed heat and small variation in sample thermal capacity. However, since the last part of the process is disregarded the N value no longer influences curve representation, thus reducing the predictive power. Moreover, it is not easy to construct a general criterion for establishing how low mass and heating rate must be or the range where W must lie, owing to their dependence on sample characteristics as well as on those of the instrumentation. Analysis of predictive power could be a good way of estimating the above limits. This may be done by lowering the mass of the sample and/or lowering the heating rate to the point where the TG curve, calculated using kinetic parameters obtained from a previous experimental curve, matches the new experimental curve satisfactory. This is not the same as looking for convergence of (Z, E, N) values which may differ in each calculation.

Even if difficult to interpret in a chemical sense, the kinetic parameters are useful for describing conditions not easily achievable as working conditions for ablating materials [3,4]. The choice of a given triplet depends on the subsequent processing of data to calculate temperatures against depth and time. If the model is complex, as reported in ref. 3 and 4 or as the CMA program (aerotherm Charring Material thermal response and Ablation) used by the U.S. Air Force Rocket Propulsion Laboratory, a better triplet would be that representing experimental data at the lowest sample mass and heating rate (as BF1). The model used for subsequent calculations takes into account mass, density, porosity, conductivity, emissivity, gas evolution, etc., so requires just an empirical description (the triplet (Z, E, N)) of the isolated reaction. If on the other hand a simple model is used, for instance eqn. (2) alone, the choice of a triplet derived from simultaneous best-fit of all available data (as BF2) would be preferred.

Finally, a suggestion to TG instrument designers: if the sample temperature could be monitored as well as the programmer temperature during experiments, or better, if the sample temperature could be controlled as in DSC, eqns. (10) or (22) could be used regardless of eqn. (18), with the possibility of describing a thermal degradation with limited influence of sample and apparatus.

REFERENCES

1 R.F. Schwenker and P.D. Garn (Eds.), Thermal Analysis Vol. 2, Academic Press, New York, 1969.

2 U. Biader Ceipidor, R. Bucci, V. Carunchio, A.M. Girelli and A.D. Magrí, J. Therm. Anal., 35(5) (1989) in press.
3 J.B. Henderson, J.A. Wiebelt and M.R. Tant, J. Compos. Mater., 19 (1985) 579.
4 J.B. Henderson and T.E. Wiecek, J. Compos. Mater., 21 (1987) 373.
5 W.W. Wendlandt, Thermal Analysis, Wiley, New York, 3rd edn, 1986.
6 L. Reich, L.Z. Pollara and S.S. Stivala, Thermochim. Acta, 111 (1987) 379.
7 A. Romero Salvador and E. García Calvo, Thermochim. Acta, 107 (1986) 283.
8 E. Urbanovici and E. Segal, Thermochim. Acta, 118 (1987) 65.
9 E. Urbanovici and E. Segal, Thermochim. Acta, 107 (1986) 353.
10 E. Urbanovici and E. Segal, Thermochim. Acta, 107 (1986) 359.
11 P.D. Garn, Thermochim. Acta, 135 (1988) 71.
12 El-H. M. Diefallah, S.N. Basahl, A.Y. Obajd and R.H. Abu-Eittah, Thermochim. Acta, 111 (1987) 49.
13 M. Tutas, M. Sağlam, M. Yüksel and Ç. Güler, Thermochim. Acta, 111 (1987) 121.
14 L. Jinxiang, Z. Quanqin, G. Xiuying, Acta Chim. Sin., 41 (2) (1983) 169.
15 E.S. Freeman and B. Carroll, J. Phys. Chem., 62 (1958) 394.
16 Z. Quanqin, L. Jinxiang and Z. Dianguo, Thermochim. Acta, 135 (1988) 187.
17 J. Šesták, Thermochim. Acta, 3 (1971) 1.